Supporting Information

Synthesis and DNA Cleavage studies of Rationally Designed Metallopeptides from N-Salicyl-AA-Picolamide (SAP) and Cu(II) Ion

Subhashree Subhadarshini Panda [a,c] , Supriya Kumari[a,b,] Manjusha Dixit [b,c] and Nagendra K Sharma,*[a.c]

[a]School of Chemical Science (SCS), National Institute of Science Education and Research (NISER), Bhubaneswar, Jatni, 752050, Odisha, India, E-mail: nagendra@niser.ac.in

[b]School of Biological Science (SBS), National Institute of Science Education and Research (NISER), Bhubaneswar, Jatani, 752050, Odisha, India

[c]Homi Bhabha National Institute (HBNI), Anushaktinagar, Mumbai, 400094, India

*Corresponding author. Tel.: 0674-249-4141; fax: +91 (674) 2494004;

Email: nagendra@niser.ac.in

Contents

1. General Procedure

Except as otherwise specified, all commercial reagents were used without further purification. Natural and unnatural amino acids, salicylic acid, Picolyl amine, DIPA, NMM, EDC.HCl and HOBt were purchased from SpectroChem and sigma Aldrich. Anhydrous DMF was purchased from Merck. Reactions were carefully monitored by thin layer chromatography (TLC), and visualized under UV or by performing ninhydrin test. Silica gel column chromatography was carried out on Merck silica gel 100-200 mesh. Nuclear magnetic resonance (NMR) spectra were recorded on Bruker 400MHz spectrometer operating at 400MHz and 101 MHz for ^{1}H and ^{13}C acquisitions, respectively. All HRMS data were recorded with a Bruker MicroTOF-Q II spectrometer. **Synthesis of N-salicyl-AAn-Picolamine Ligands and Cu- Complex**

*Synthesis of ligands **3a-3d**:-* N-salicyl-AAn-Picolamine ligands (**3a-3d**) has been synthesized according to the literature.

*Synthesis of Cu Complex **4a-4d**:-* N-salicyl-AAn-Picolamine ligands (**3a-3d**) (1eq each) was solubilized in 1:1 ratio of MeOH and DCM. Then 1eq $Cu(OAc)_2$ solution in methanol was added dropwise (Scheme S1). Then reaction mixtures were kept undisturbed to get needle shape crystals. Then crystals of each peptide (**4a-4d**) were washed with methanol and diethyl ether and characterised by mass spectrometry.

Scheme S1. Observation of complex formation

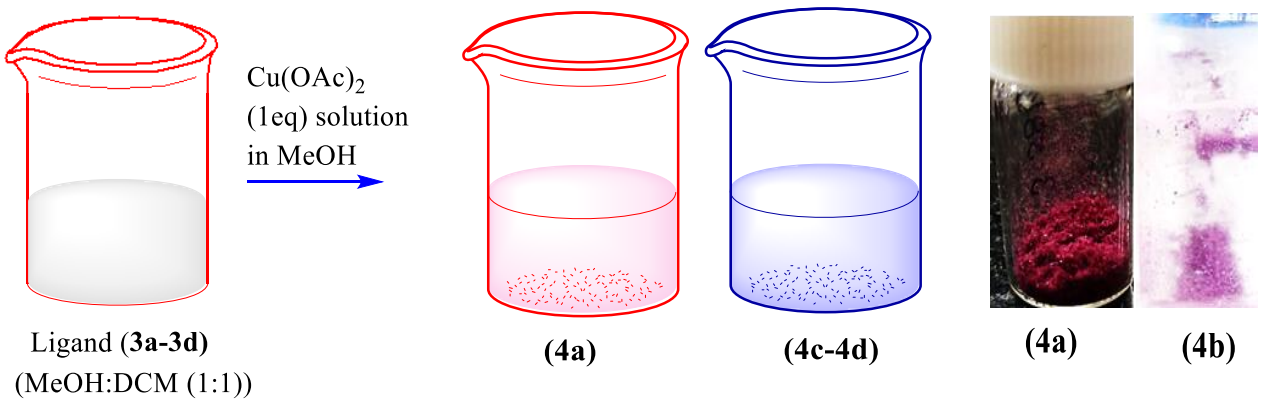

TABLE-S1. Calculated and found m/z values in ESI-MS of prepared Cu- complex **4a-4d**

COMPOUND	**4a**	**4b** ($C_{16}H_{16}CuN_3O_3$ $[M+H]^+$)	**4c**	**4d**
CALCULATED	347.0331	361.0488	389.0801	403.0957
FOUND	347.0327	361.0496	389.0762	403.0922

2. ESI-HRMS spectra of Cu Complex

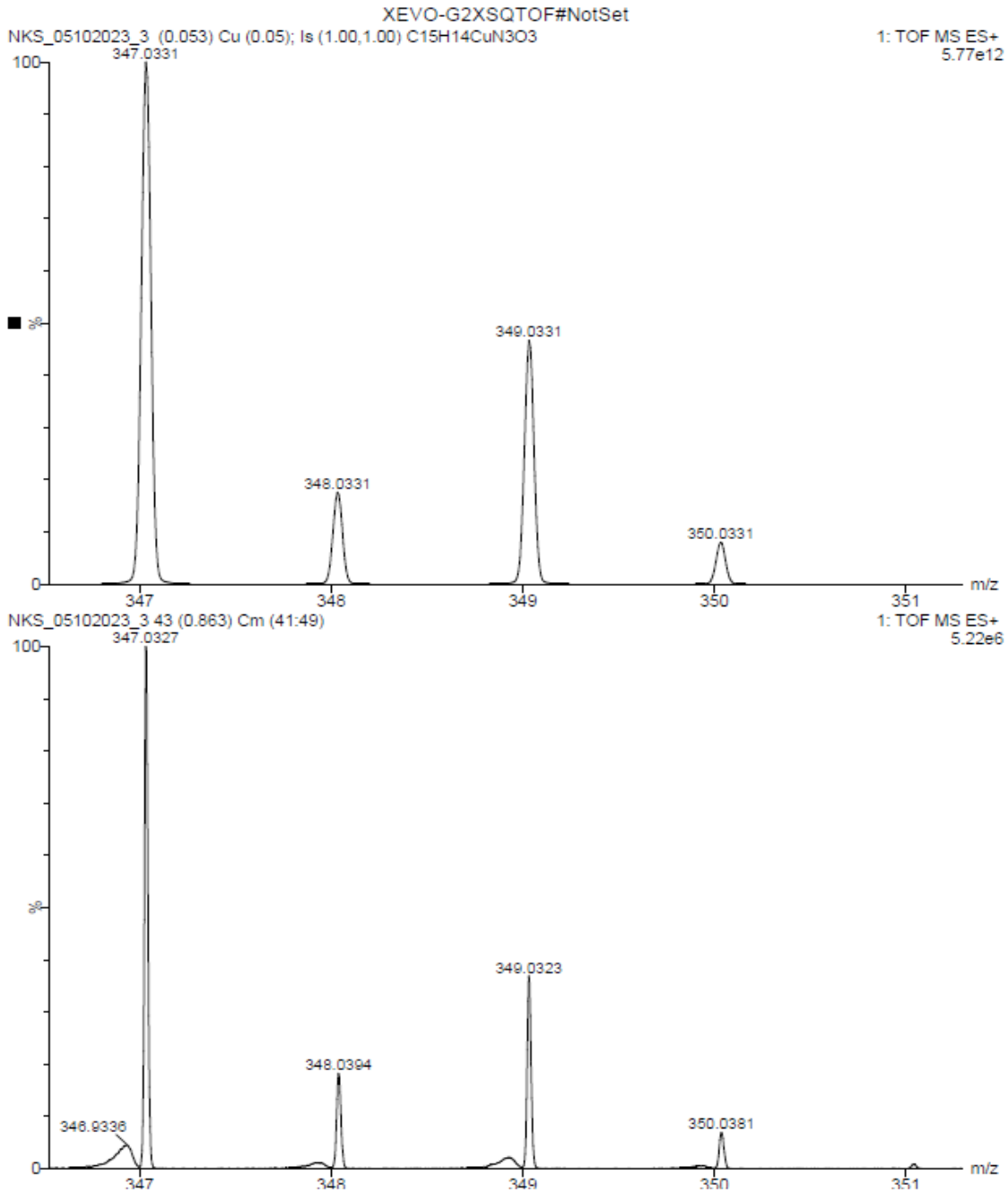

Figure S1. ESI-HRMS spectra of Cu Complex **4a**, Calculated (above) and Observed (below).

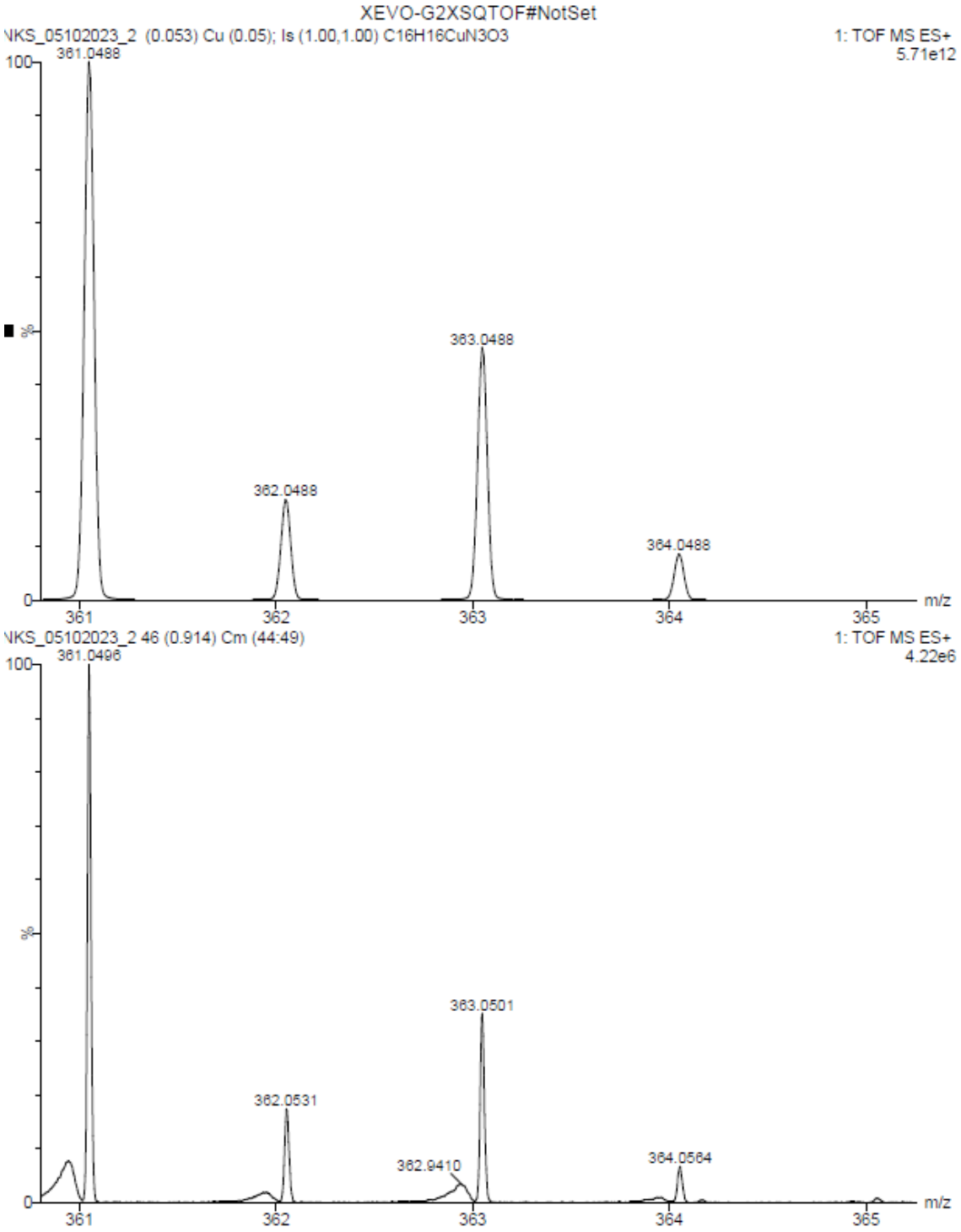

Figure S2. ESI-HRMS spectra of Cu Complex **4b,** Calculated (above) and Observed (below)

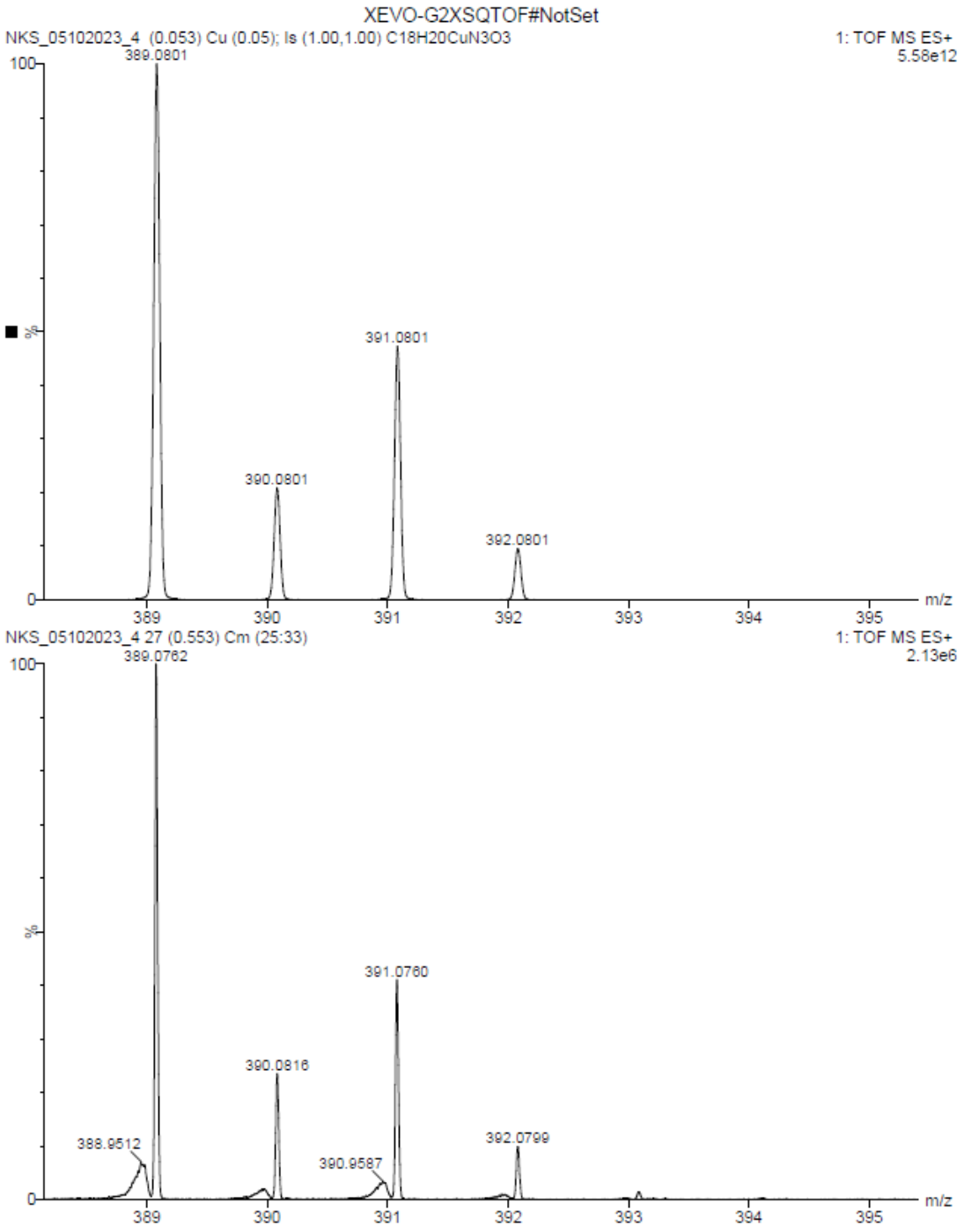

Figure S3. ESI-HRMS spectra of Cu Complex **4c,** Calculated (above) and Observed (below)**.**

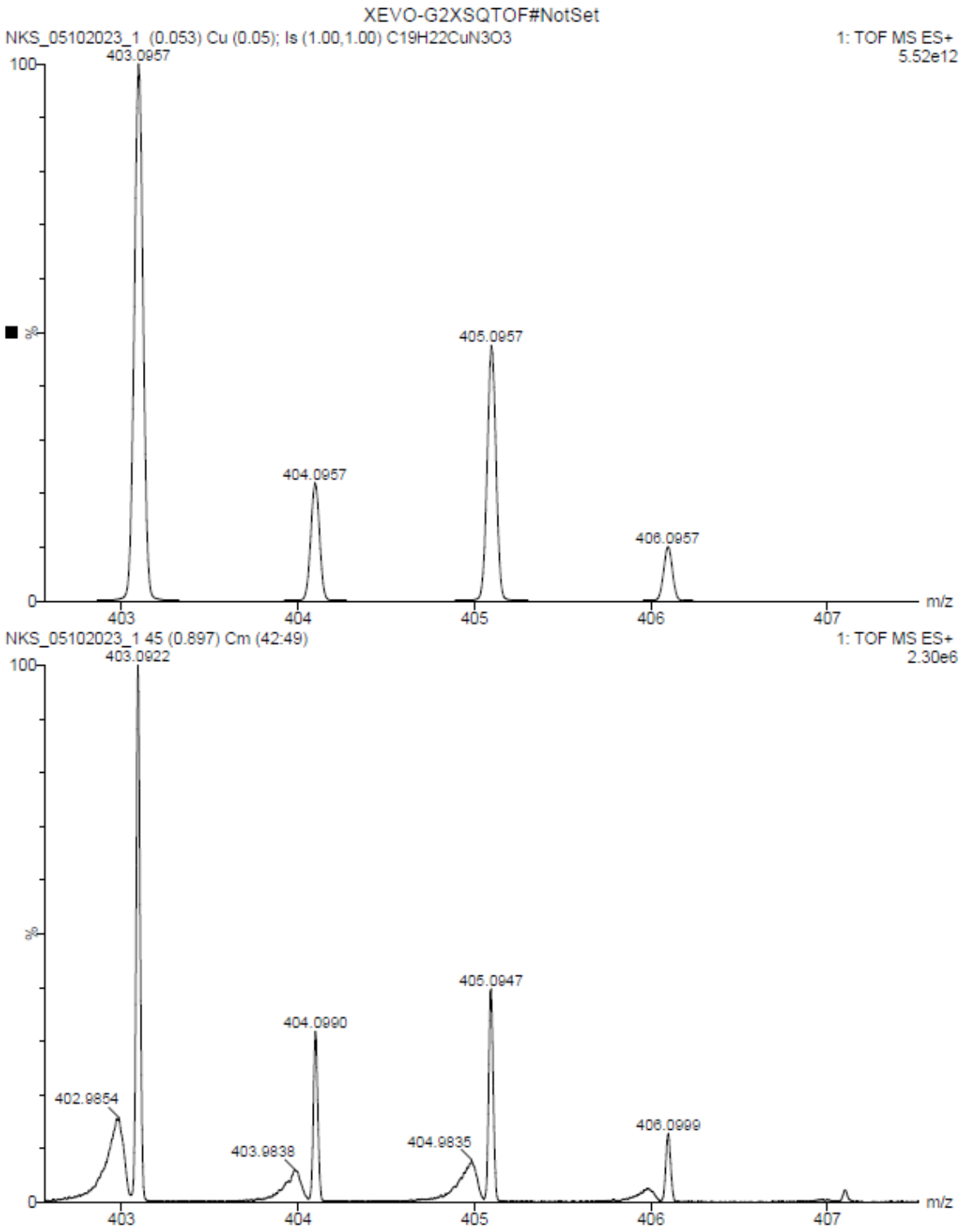

Figure S4. ESI-HRMS spectra of Cu Complex **4d**, Calculated (above) and Observed (below).

3. FTIR Spectra of Ligands 3a-3d & Cu complex 4a-4d

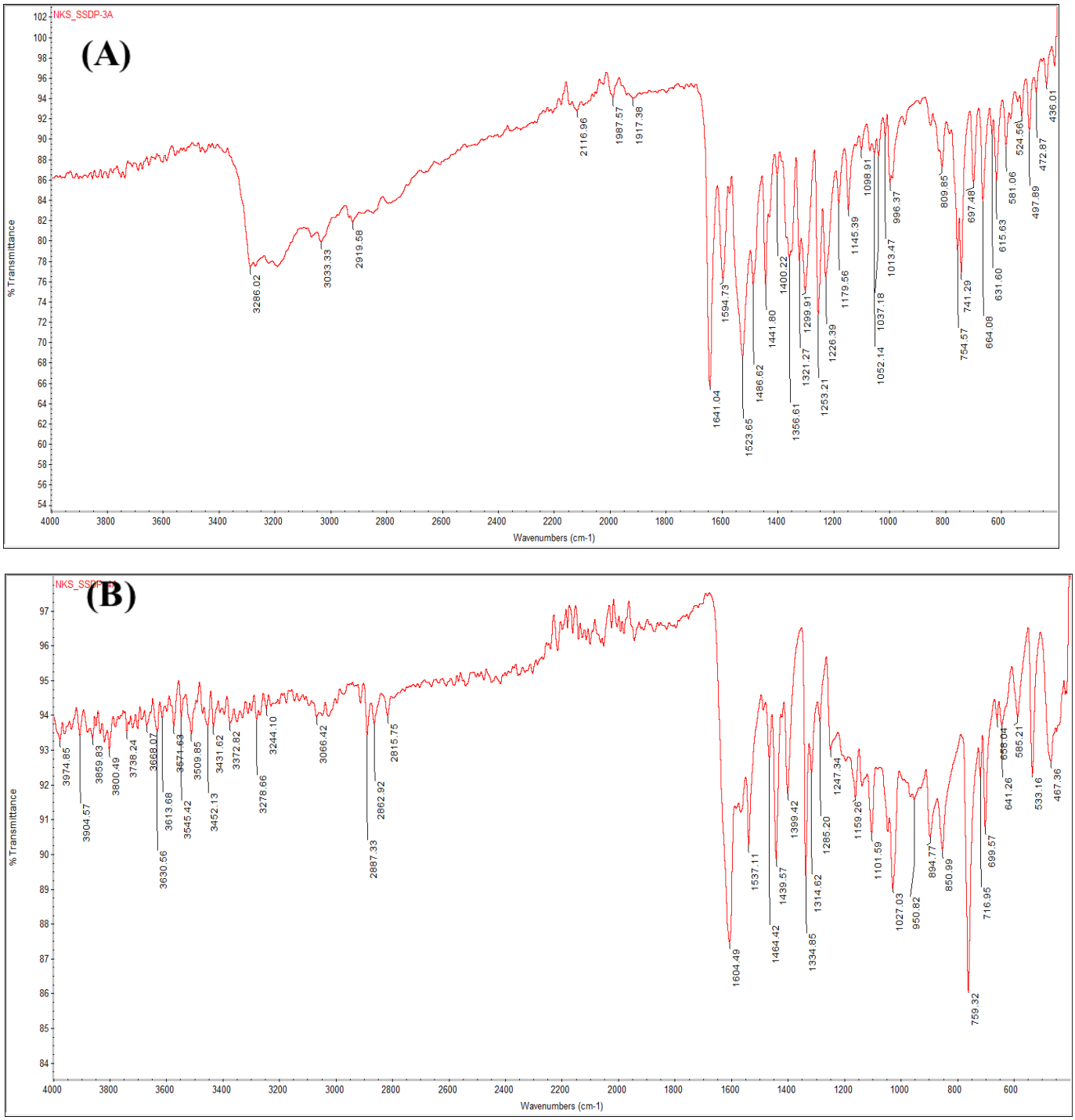

Figure S5. (A) FTIR Spectra of Ligands **4a;** (B)FTIR Spectra of Cu complex **4a.**

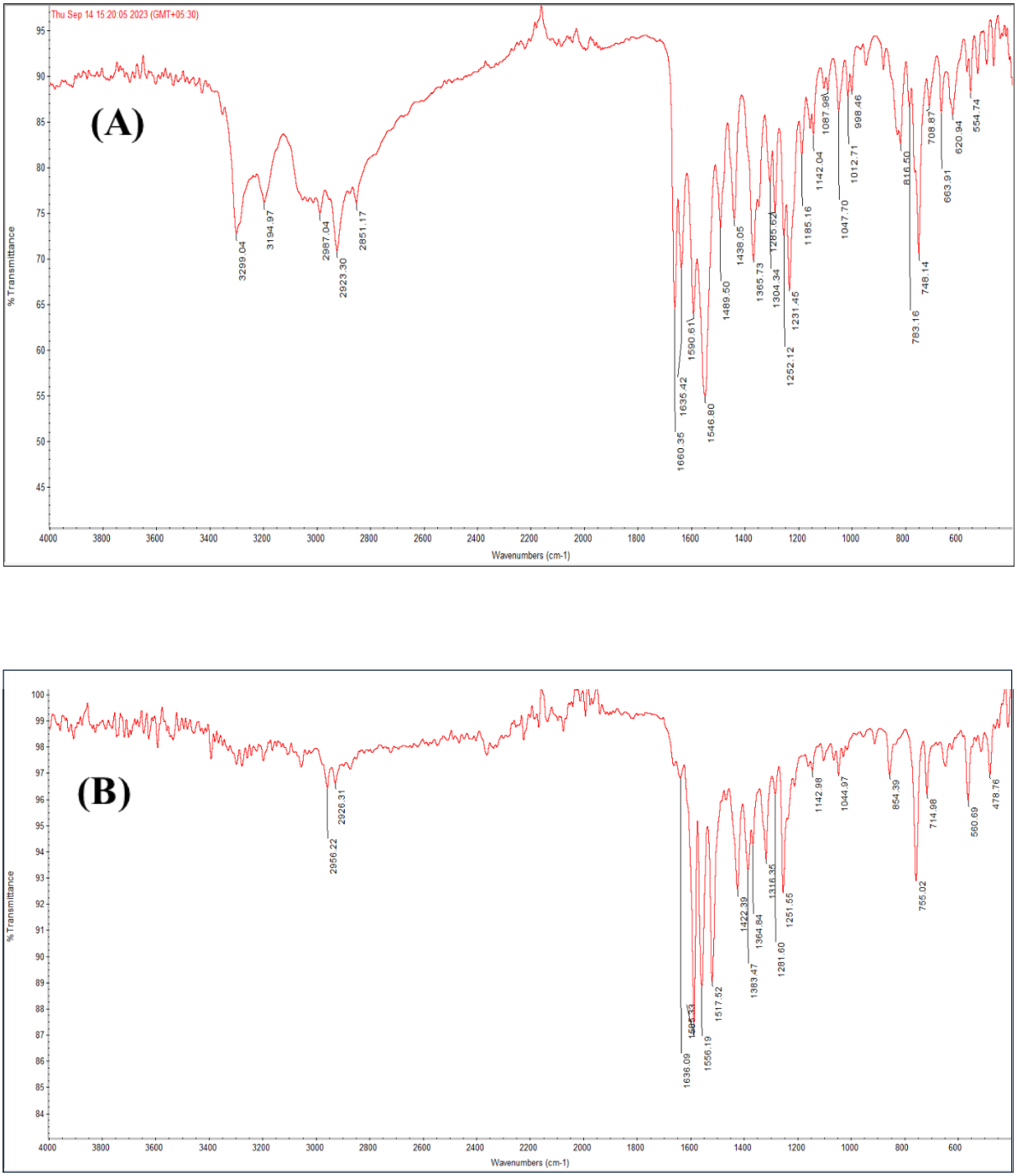

Figure S6. (A) FTIR Spectra of Ligands **4b** & (B)FTIR Spectra of Cu complex **4b.**

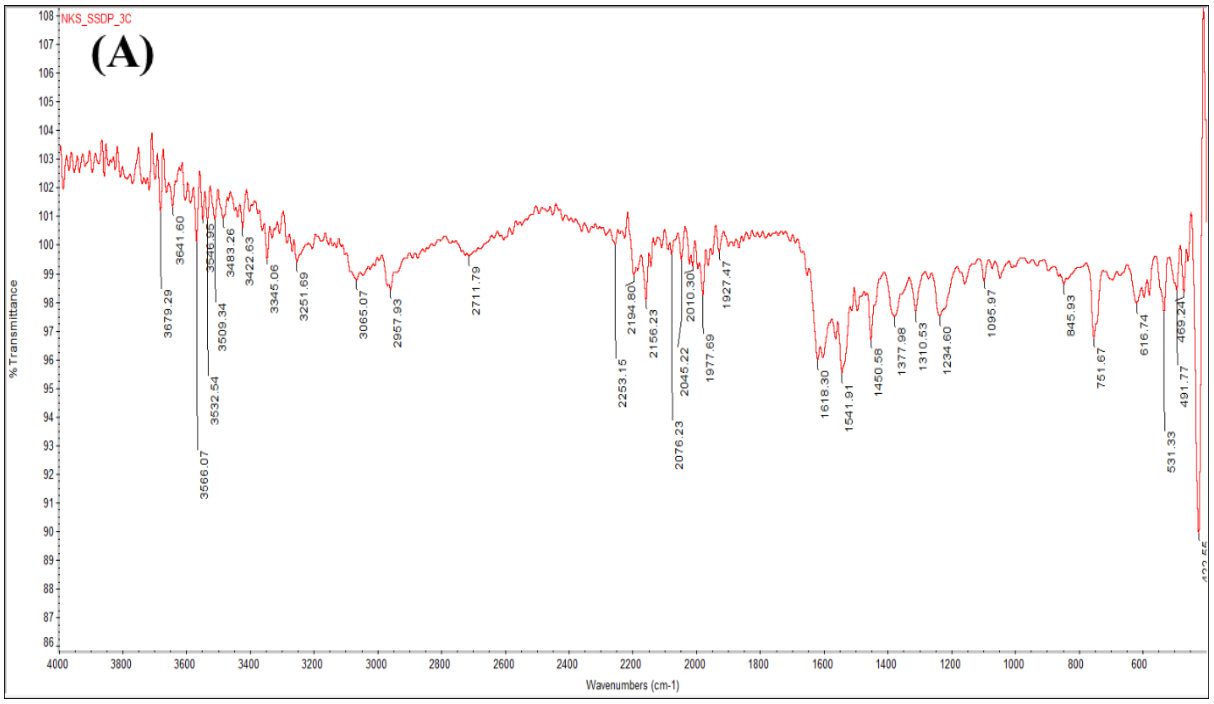

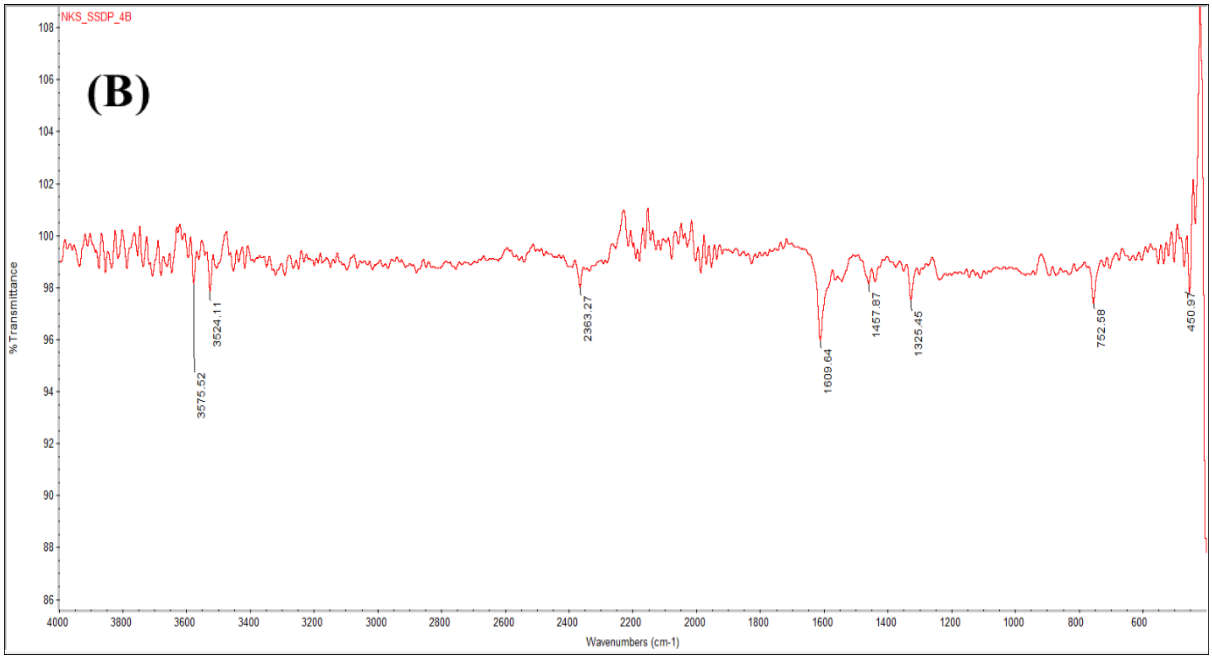

Figure S7. (A) FTIR Spectra of Ligands **4c** & (B)FTIR Spectra of Cu complex **4c.**

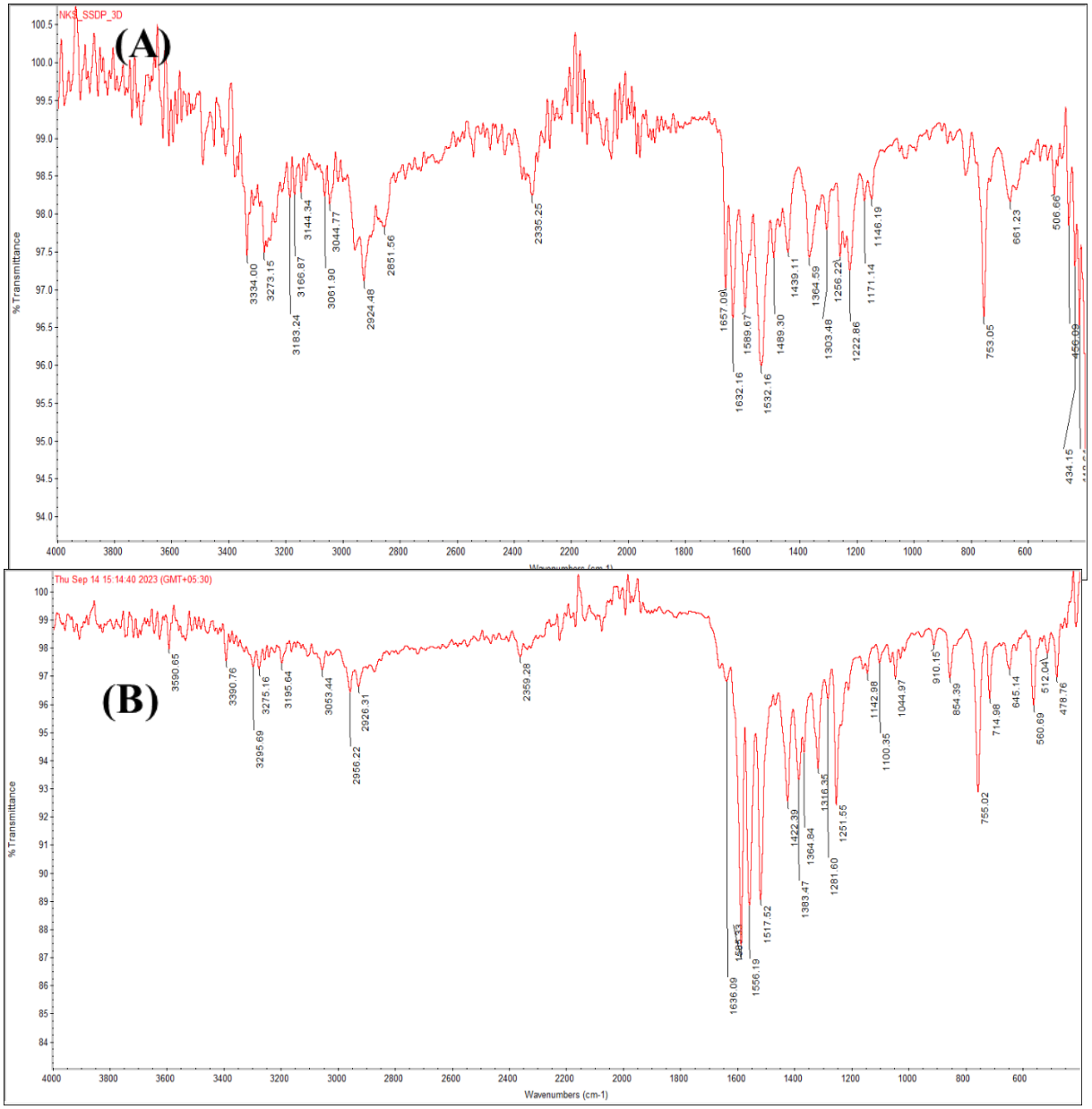

Figure S8. (A) FTIR Spectra of Ligands **4d** & (B)FTIR Spectra of Cu complex **4d.**

4. EPR Spectra of Ligands 3a-3d & Cu complex 4a-4d

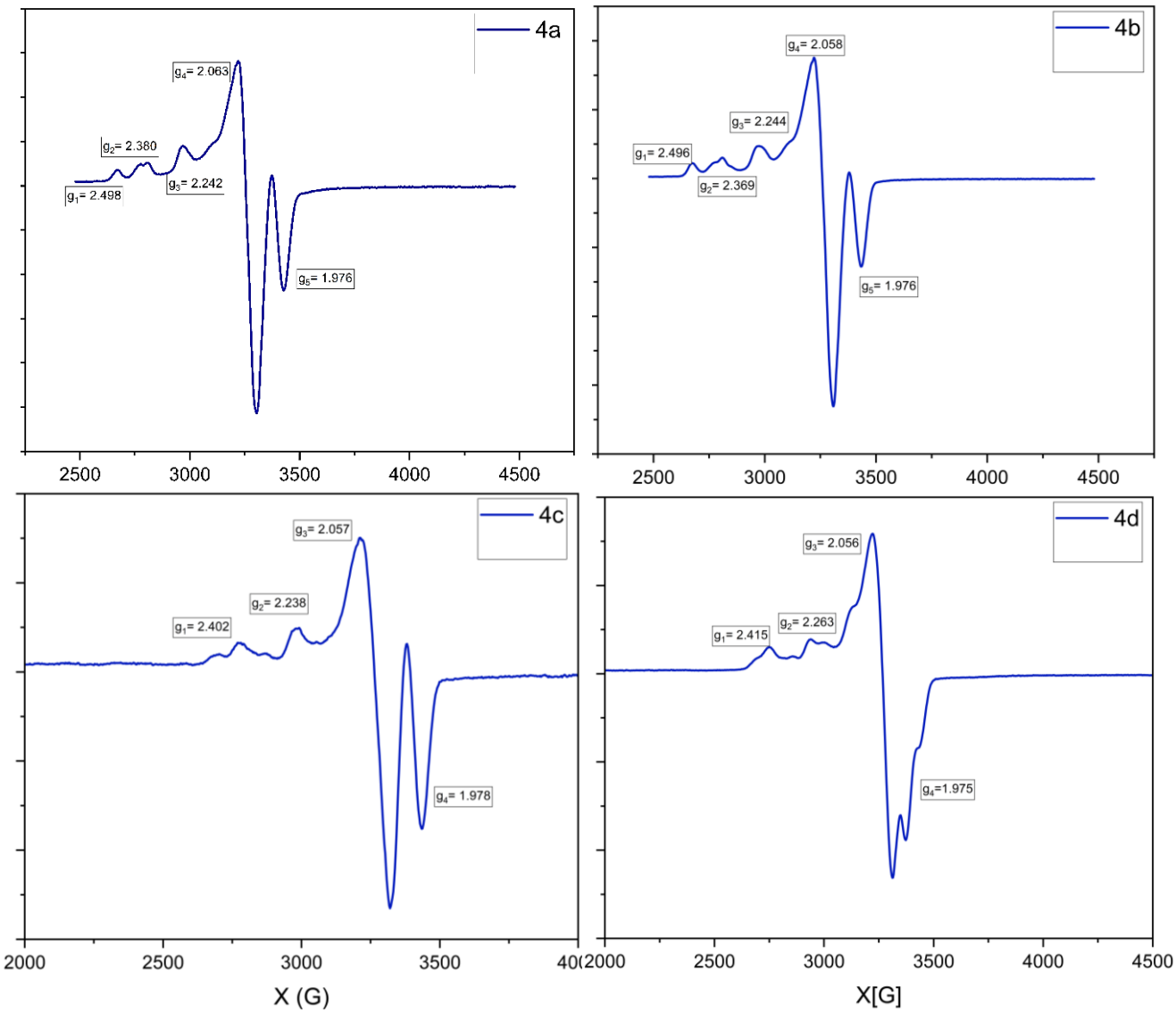

Figure S9. EPR Spectra of Ligands 3a-3d & Cu complex **4a-4d**.

5. X-Ray Crystal structure of Cu complex 4a-4c.

The crystal data of all peptides Cu complexes were collected on Rigaku Oxford diffractometer at 293 K respectively. SHELXT1 and Olex2 software was used for structure solution and packing diagram carried out by DIAMOND-3.3 software.

Table S2. *Crystal data and structure refinement for peptide* ***4a (CCDC No*-2326996)**

Identification code	***4a (CCDC No*-2326996)**
Empirical formula	$C_{15}H_{13}CuN_3O_3$
Formula weight	346.83
Temperature/K	297.15
Crystal system	monoclinic
Space group	$P2_1/c$
a/Å	11.3112(9)
b/Å	6.6485(5)
c/Å	18.4942(14)
α/°	90
β/°	104.164(8)
γ/°	90
Volume/Å^3	1348.53(19)
Z	4
ρ_{calc}g/cm^3	1.7082
μ/mm^{-1}	1.636
F(000)	709.6
Crystal size/mm^3	0.31 × 0.22 × 0.18
Radiation	Mo Kα (λ = 0.71073)
2Θ range for data collection/°	7.16 to 52.72
Index ranges	$-14 \leq h \leq 14$, $-8 \leq k \leq 8$, $-23 \leq l \leq 23$
Reflections collected	12828
Independent reflections	2748 [R_{int} = 0.0586, R_{sigma} = 0.0488]
Data/restraints/parameters	2748/0/200
Goodness-of-fit on F^2	1.029
Final R indexes [I>=2σ (I)]	R_1 = 0.0319, wR_2 = 0.0783
Final R indexes [all data]	R_1 = 0.0381, wR_2 = 0.0814
Largest diff. peak/hole / e Å^{-3}	0.37/-0.35

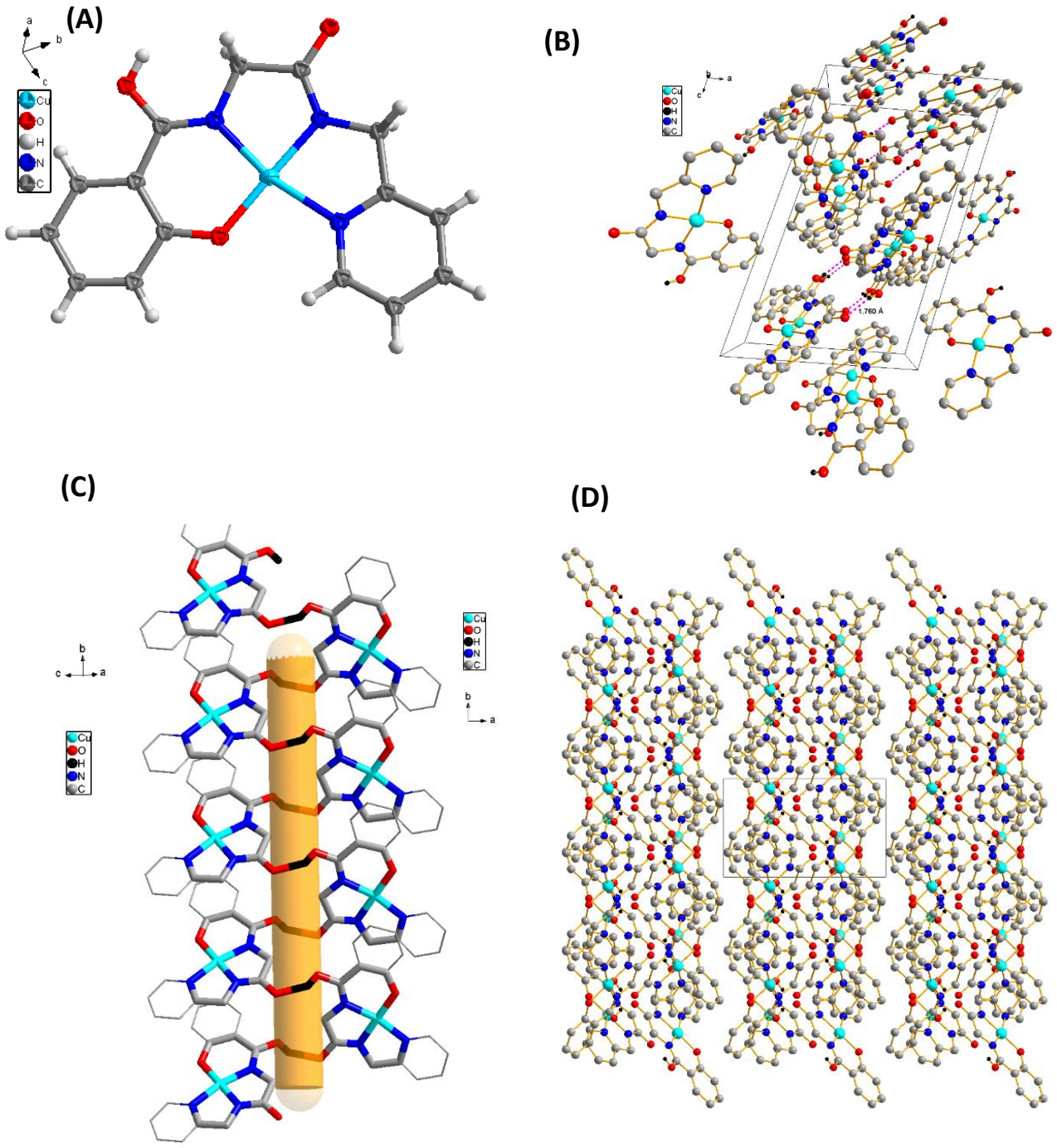

Figure S10. Structural analysis of SAP's Cu complex **4a** (A) ORTEP Diagram of **4a** (B-D) Structure and unit cell packing diagram of **4a.**

Table S3. Crystal data and structure refinement for Cu complex **4b (CCDC No-232699**

Identification code	**4b *(CCDC No*-2326997)**
Empirical formula	$C_{16}H_{14}CuN_3O_3$
Formula weight	360.86
Temperature/K	298.15
Crystal system	triclinic
Space group	P-1
a/Å	7.2629(2)
b/Å	10.8594(4)
c/Å	11.3480(4)
α/°	114.939(4)
β/°	104.016(3)
γ/°	96.535(3)
Volume/Å^3	763.32(6)
Z	2
ρ_{calc}g/cm^3	1.5699
μ/mm^{-1}	1.449
F(000)	370.8
Crystal size/mm^3	0.01 × 0.01 × 0.002
Radiation	Mo Kα (λ = 0.71073)
2Θ range for data collection/°	7.14 to 52.74
Index ranges	$-9 \leq h \leq 10$, $-14 \leq k \leq 14$, $-15 \leq l \leq 15$
Reflections collected	17422
Independent reflections	3109 [R_{int} = 0.0413, R_{sigma} = 0.0299]
Data/restraints/parameters	3109/0/211
Goodness-of-fit on F^2	1.040
Final R indexes [I>=2σ (I)]	R_1 = 0.0251, wR_2 = 0.0642
Final R indexes [all data]	R_1 = 0.0273, wR_2 = 0.0654
Largest diff. peak/hole / e Å^{-3}	0.32/-0.28

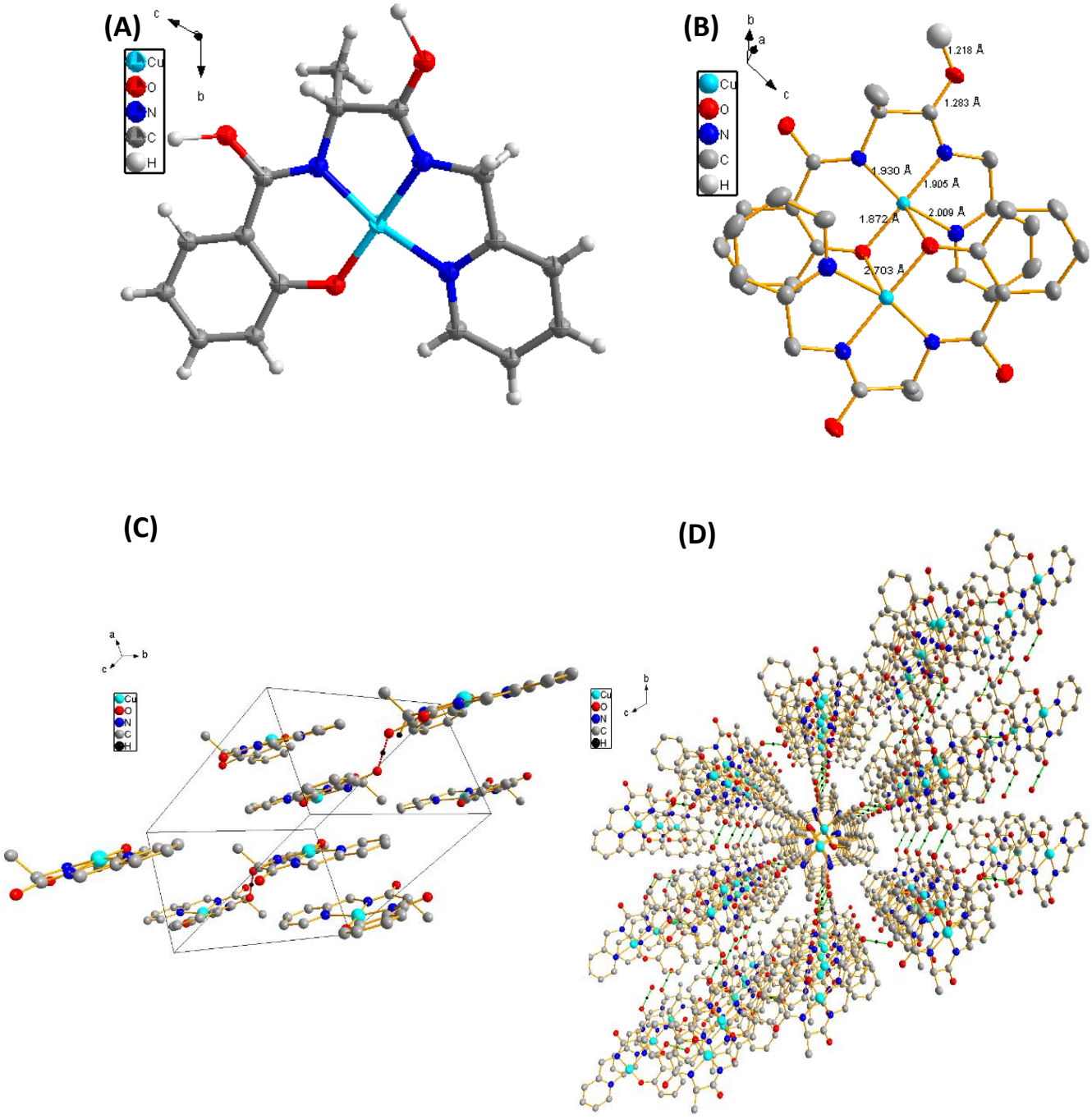

Figure S11. Structural analysis of SAP's Cu complex 4b (A) ORTEP Diagram of **4b** (B-D) Structure and unit cell packing diagram of **4b.**

Table S4. Crystal data and structure refinement for Cu complex **4C (CCDC No-2326998).**

Table S8	
Identification code	**4c *(CCDC No*-2326998)**
Empirical formula	$C_{3.13}H_{3.3}Cu_{0.17}N_{0.52}O_{0.52}$
Formula weight	67.637
Temperature/K	296
Crystal system	monoclinic
Space group	$P2_1/n$
a/Å	7.3019(1)
b/Å	13.8300(2)
c/Å	16.2105(2)
α/°	90
β/°	94.256(1)
γ/°	90
Volume/Å^3	1632.51(4)
Z	23
ρ_{calc}g/cm^3	1.582
μ/mm^{-1}	2.090
F(000)	798.6
Crystal size/mm^3	0.1 × 0.01 × 0.01
Radiation	Cu Kα (λ = 1.54184)
2Θ range for data collection/°	8.42 to 156.42
Index ranges	$-8 \le h \le 6$, $-16 \le k \le 17$, $-20 \le l \le 20$
Reflections collected	13438
Independent reflections	3368 [R_{int} = 0.0405, R_{sigma} = 0.0320]
Data/restraints/parameters	3368/0/229
Goodness-of-fit on F^2	1.028
Final R indexes [I>=2σ (I)]	R_1 = 0.0341, wR_2 = 0.0970
Final R indexes [all data]	R_1 = 0.0367, wR_2 = 0.0996
Largest diff. peak/hole / e Å^{-3}	0.26/-0.46

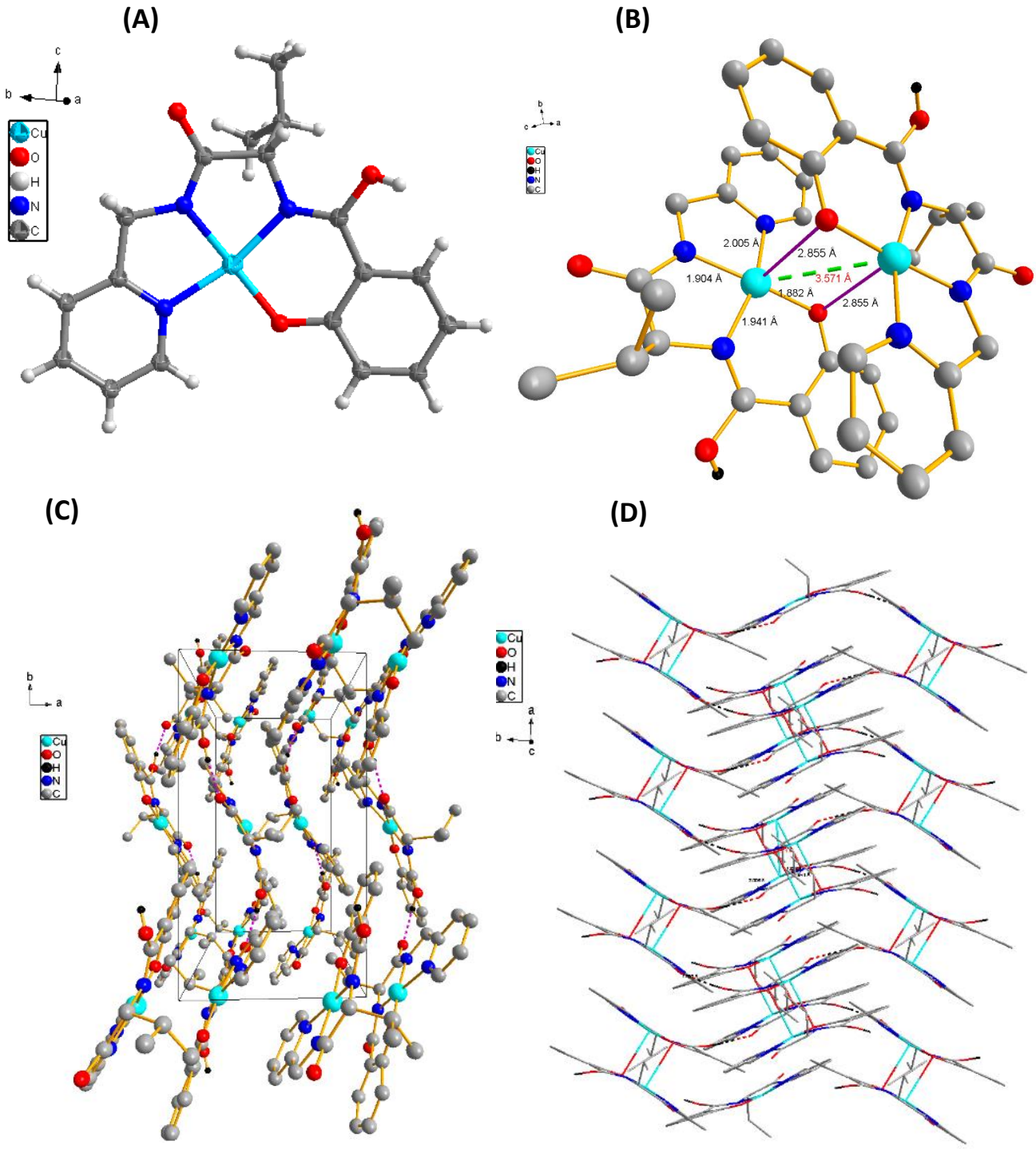

Figure S12. Structural analysis of SAP's Cu complex 4c (A) ORTEP Diagram of **4c** (B-D) Structure and unit cell packing diagram of **4c.**

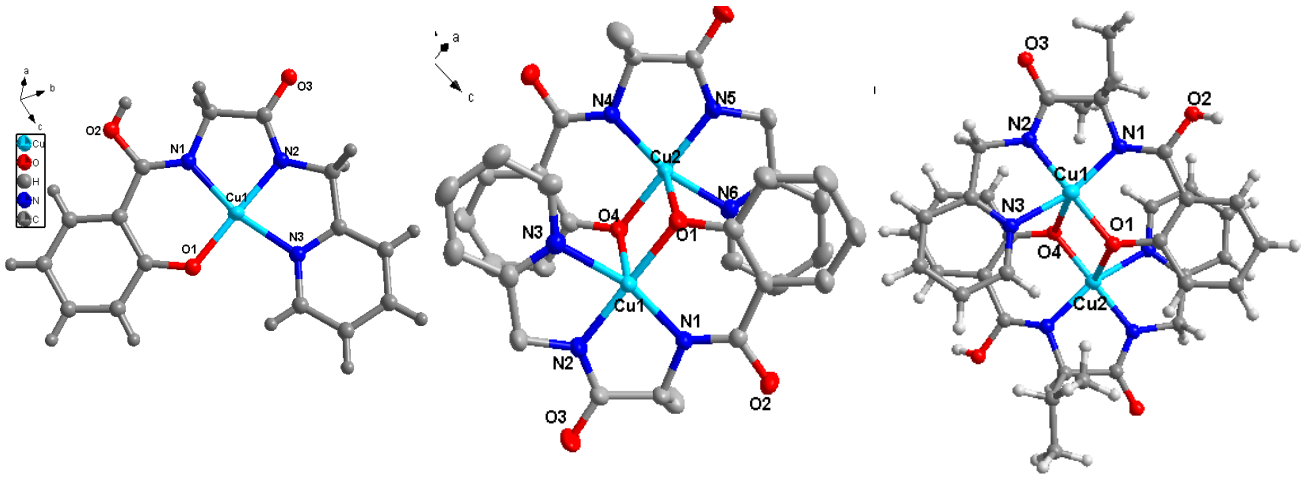

(4a) **(4b)** **(4c)**

Figure S13. X-ray structure of the Cu (II) complexes (**4a, 4b, 4c**).

Table S5. Selected structural parameters observed in the solid-state structure of **4a, 4b,4c**.

Bond Length (Å)		**Bond Angle (°)**	
For complex **4a**			
Cu1-N1	1.933	N1-Cu1-O2	96.827
Cu1-N2	1.904	N1-Cu1-N2	84.149
Cu1-N3	1.997	N1-Cu1-N3	82.115
Cu1-O1	1.860		
For complex **4b**			
Cu1-N1	1.930	O1-Cu1-N1	96.696
Cu1-N2	1.905	N1-Cu1-N2	83.752
Cu1-N3	2.009	N2-Cu1-N3	81.962
Cu1-O1	1.872	O1-Cu1-O4	85.406
Cu1-O4	2.703	Cu1-O4-Cu2	94.594
For complex **4c**			
Cu1-N1	1.941	O1-Cu1-N1	96.549
Cu1-N2	1.904	N1-Cu1-N2	83.906
Cu1-N3	2.005	N2-Cu1-N3	82.312
Cu1-O1	1.882	Cu1-O4-Cu2	95.644

Cu1-O4	2.855	O1-Cu1-O4	84.356

6. Scanning Electron Microscopy (SEM)

A thin layer sample of Cu-complex 4a,4b, 4c & 4d were prepared from dropping of EtOH mixture of these samples on silicon wafer and then we recorded their SEM image. SEM images in nano-scales, at selectively resolution (1-100um) are illustrated in **Figure (S8-S11).**

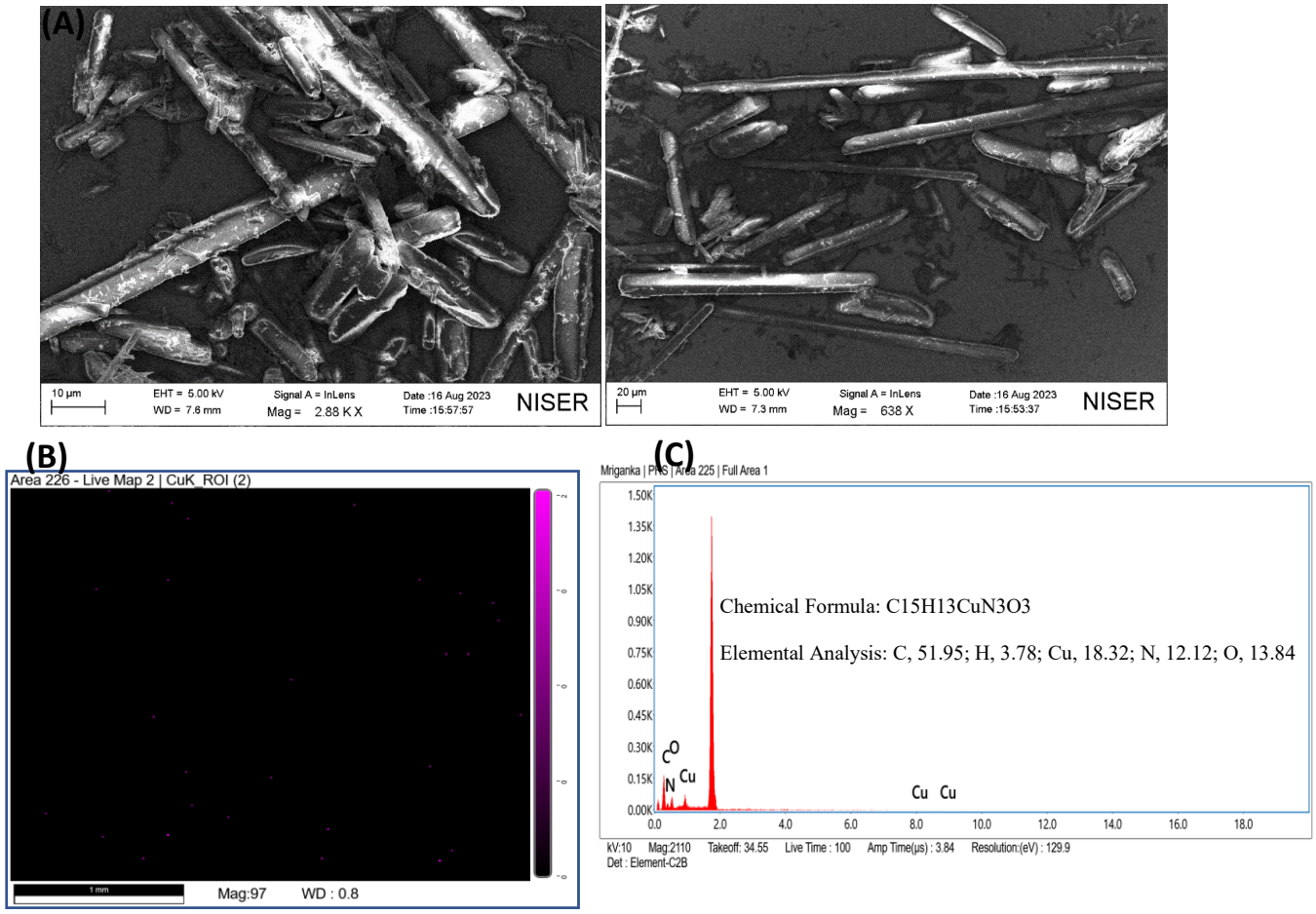

Figure S14. (A) SEM image of **4a** (B-C) Mapping & EDAX spectra of **4a**

Table S6. Elemental analysis **4a**.

Element	Weight %	Atomic %	Net Int.
C K	41.20	54.30	11.10
N K	17.70	20.00	2.00
O K	20.80	20.60	3.80
Cu L	20.30	5.10	2.80

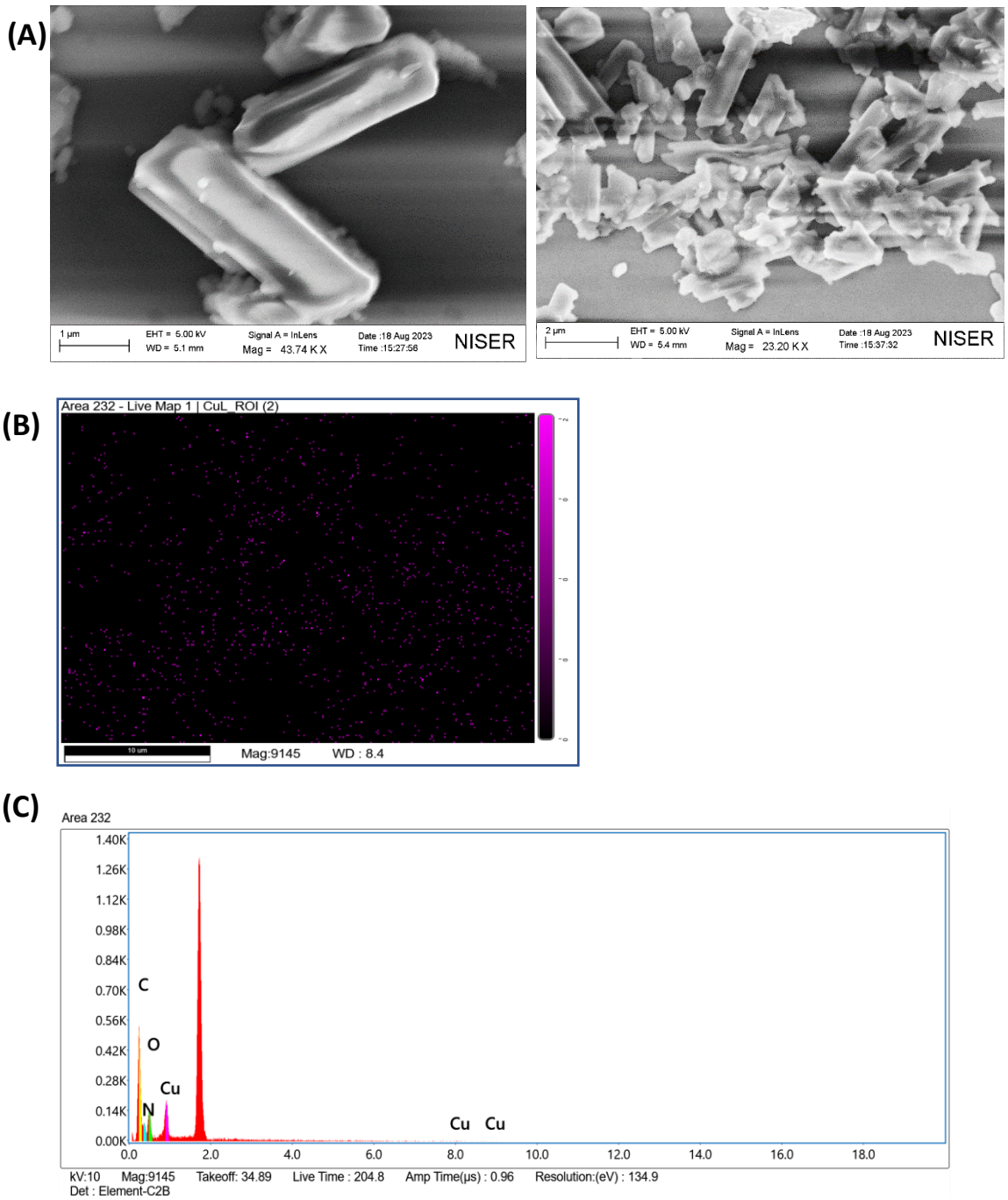

Figure S15. (A) SEM image of **4b** (B) Mapping & EDAX spectra of **4b**

Table S7. . Elemental analysis **4b**.

Element	Weight %	Atomic %	Net Int.
C K	46.20	60.90	20.20
N K	15.70	17.70	2.60
O K	16.10	15.90	4.60
Cu L	22.10	5.50	5.10

(A)

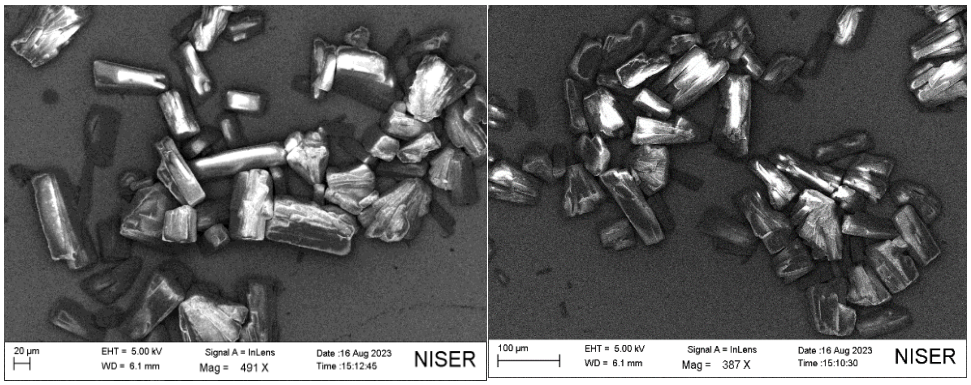

(B)

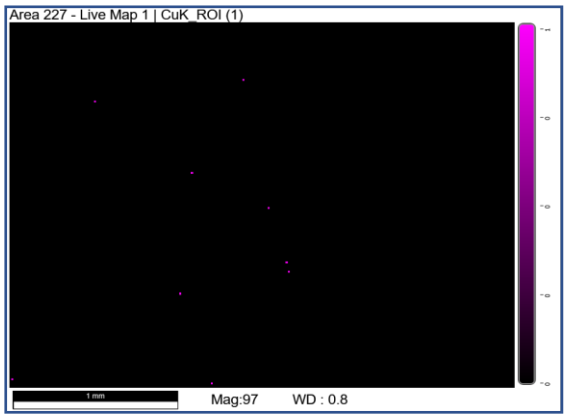

(C)

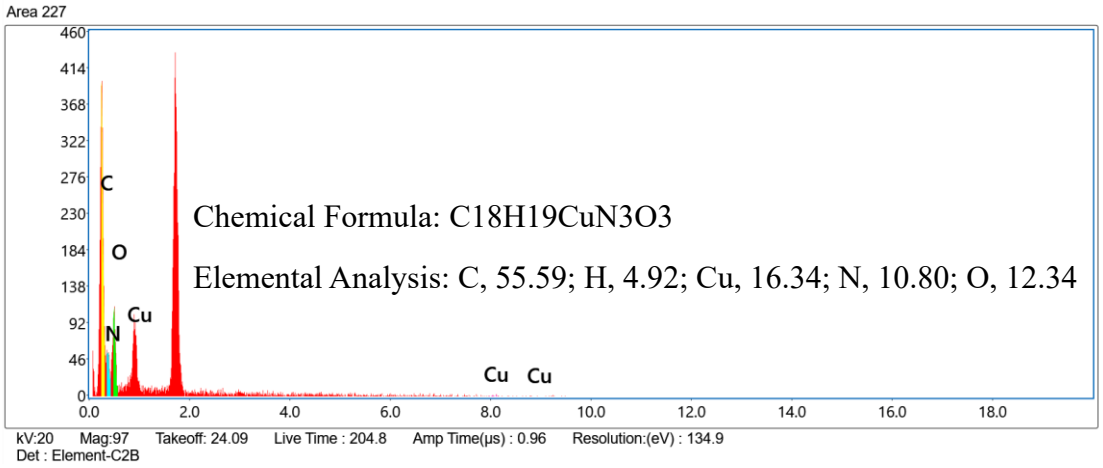

Figure S16. (A) SEM image of **4c** (B) Mapping & EDAX spectra of **4c.**

Table S8. . Elemental analysis **4c**

Element	**Weight %**	**Atomic %**	**Net Int.**
C K	46.60	52.30	15.50
N K	24.50	23.60	1.80
O K	28.60	24.10	3.30
Cu K	0.30	0.10	0.10

(A)

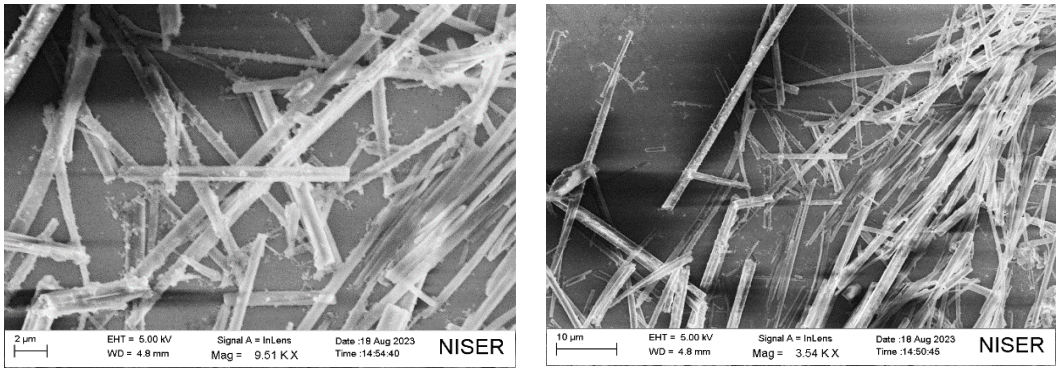

(B)

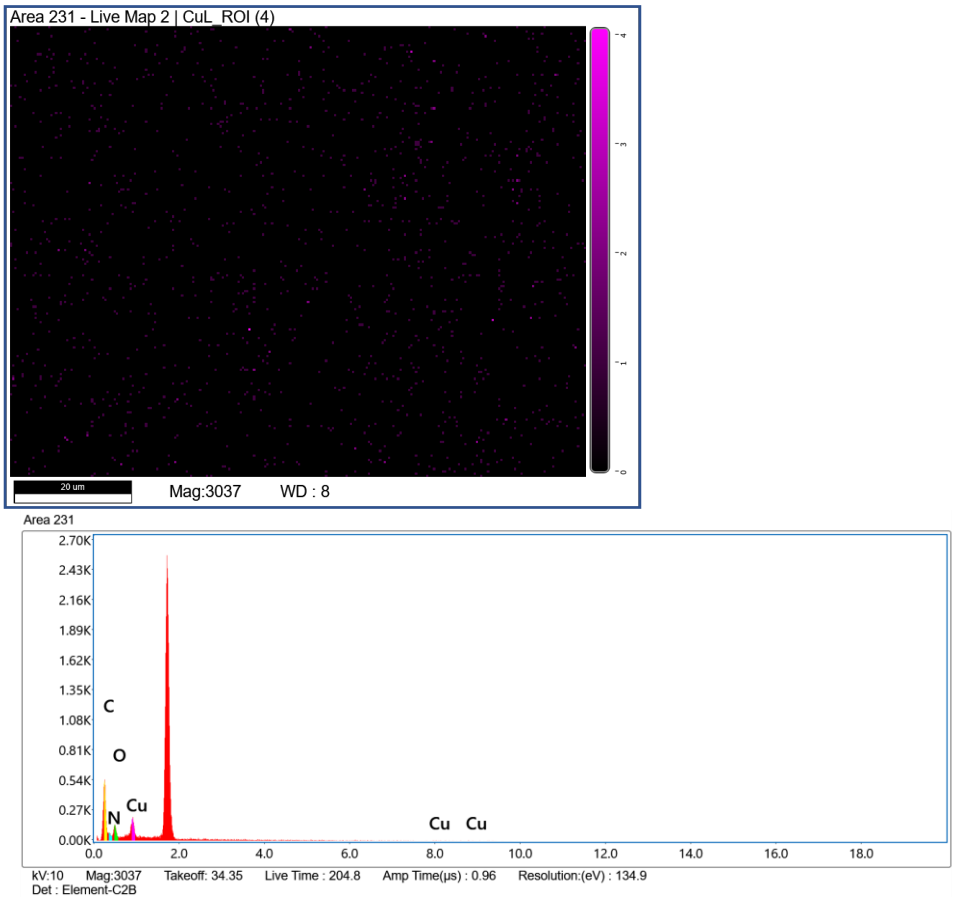

Figure S17. (A) SEM image of **4d** (B) Mapping & EDAX spectra of **4d**

Table S9. . Elemental analysis **4d**.

Element	Weight %	Atomic %	Net Int.
C K	49.70	65.60	20.20
N K	12.70	14.40	1.80
O K	14.40	14.20	3.90
Cu L	23.30	5.80	5.10

7. DNA Cleavage Assay

The study investigated the ability of copper (II) complexes to cleave pcDNA 3.1 myc plasmid DNA (100ng) when hydrogen peroxide (250 mM) was present as an activator. This was done using agarose gel electrophoresis in a 10 mM Tris–HCl/50 mM NaCl buffer (pH 7.4) at 37°C. The competence of the complexes as nucleases was assessed by their capacity to convert supercoiled DNA (form I) into nicked circular DNA (form II) and further into linear DNA (form III), which migrate at different rates in the gel. Over time, the complexes demonstrated an increasing ability to cleave the DNA, leading to a gradual reduction in the quantity of pcDNA 3.1 myc plasmid DNA. The control in lane 1 showed no cleavage of the supercoiled DNA when no complex was added. Plasmid DNA incubated with complex alone (lanes 7-10) did not alter the supercoiled form. However, in the presence of hydrogen peroxide (H_2O_2), the copper (II) complexes were able to cleave the supercoiled plasmid DNA (Lane 3-6). The distribution of supercoiled, nicked circular, and linear forms of DNA in the agarose gels provide insight into the extent of DNA cleavage by these complexes.

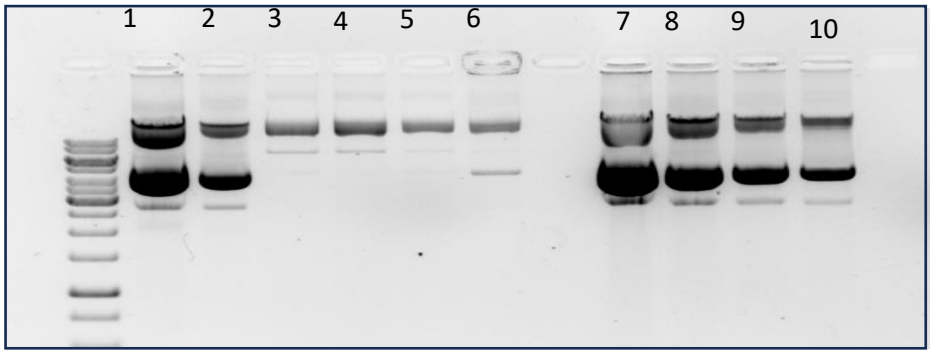

Figure S18. Lane (1) pcDNA3.1 myC (100 ng), Lane (2) pcDNA3.1 myC (100 ng) + H_2O_2 (250µM), Lane (3-6) pcDNA3.1 myC (100 ng) + H_2O_2(250µM) + **4a-4d,** Lane (7-10) pcDNA3.1 myC (100 ng) +**4a-4d.**

Time course of the DNA cleavage activity of Cu complex

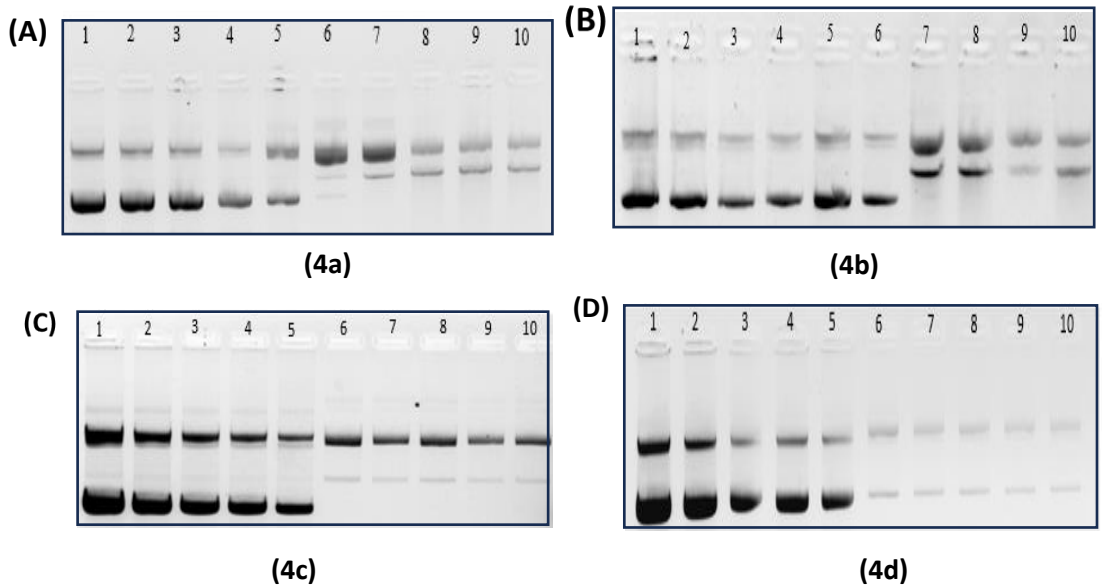

Figure S19. (Lane 1-10) pcDNA3.1 myC (100 ng) + H_2O_2 (250µM) +**4a-4d** (0,5, 15, 30, 45, 60, 90, 120, 150, 180 min)

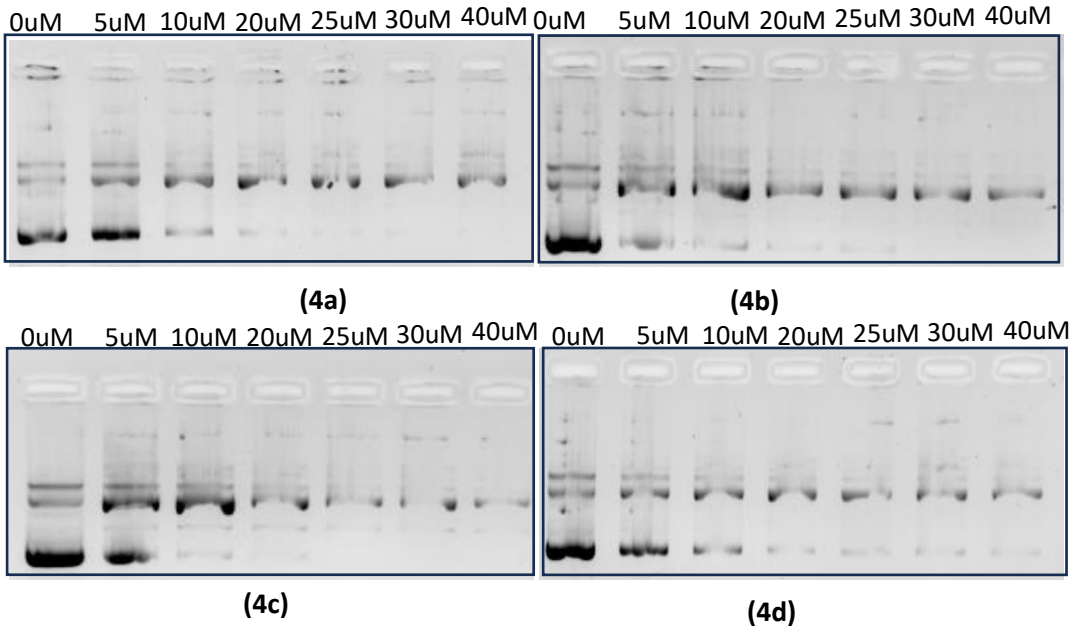

Figure S20 pcDNA3.1 myC (100 ng) + Ascorbic Acid (250µM) +**4a-4d** (0-40µm) after incubation time of 30min at 37℃.

8. Cell proliferation assay of SAP's Cu complexes

In this experiment, two cell lines, Hek293T and HeLa cells, were cultured in a 96-well microtiter plate in 10% DMEM. After a 10-hour incubation, the medium was aspirated, and cell morphology and confluency were examined. SAP's Cu complex solutions at various concentrations, along with media and a DMSO control, were added in triplicate to the wells. The plate was then incubated for 24 hours in a standard condition (humid incubator, 5% CO_2, 37°C). To assess cell proliferation, CellTiter 96® Aqueous One Solution reagent (10µl) was added to each well containing the samples in 190µl of culture medium. The plate was incubated for an additional hour under standard conditions. After incubation, absorbance was measured at 490 nm using the Varioskan Flash multimode method. This analysis provided insights into the cell proliferation ability in the presence of different peptide concentrations, with the controls serving as references for comparison.

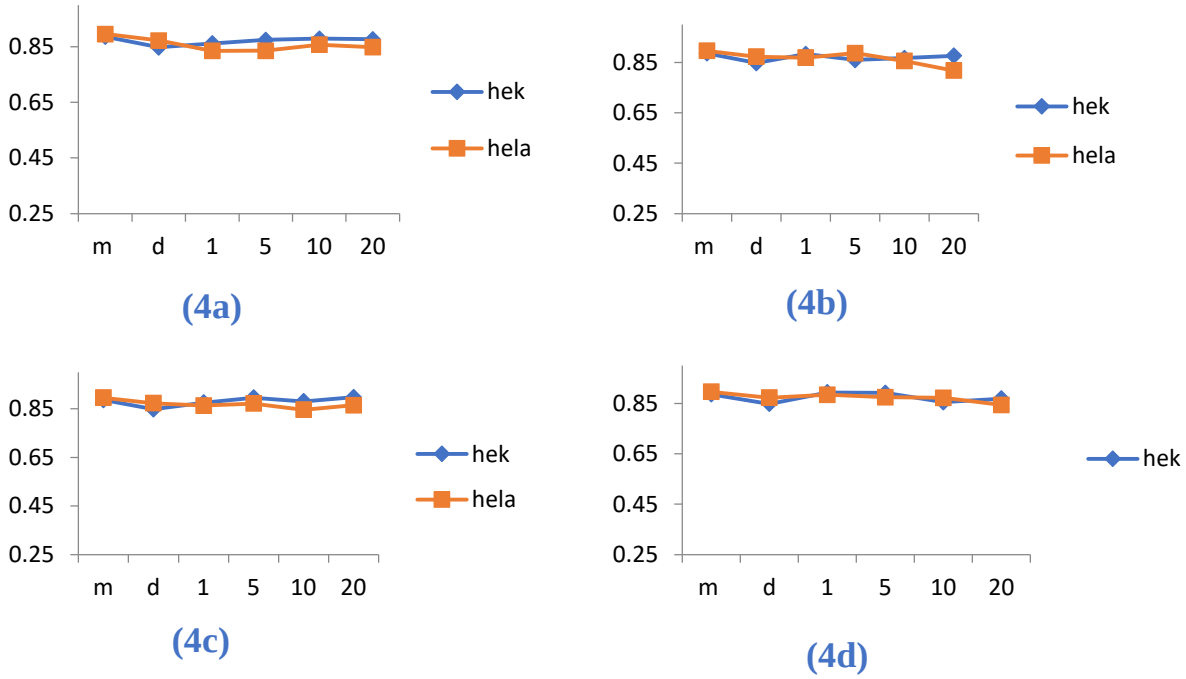

Figure S21. Cell viability of Hela cells and Heck 293T cells after incubation with SAPs Cu complexes **4a-4d.**

9. **Theoretical Molecular docking studies**

We performed molecular docking with two SAP-Cu complexes with reported DNA duplex structure (PDB ID 1BNA) using freely available AutoDock Vina software.[1] Their interactions are viewed by the molecular modeling software PyMol. The molecular model of SAP-Cu (3a-Cu) shows that complex bind with DNA in a minor groove site with binding affinity -8.1 kcal/mol through two hydrogen bonding (~2.8Å) with two guanine residue. However, the molecular model of SAP-Cu (3c-Cu) shows that complex bind with DNA in minor groove site with binding affinity -7.9 kcal/mol through two hydrogen bonding (~2.8Å) with one guanine and backbone 2'-O oxygen residue.

(a) Docking of Complex **4a** (SAP3c-Cu**) with** DNA duplex structure (PDB ID 1BNA).

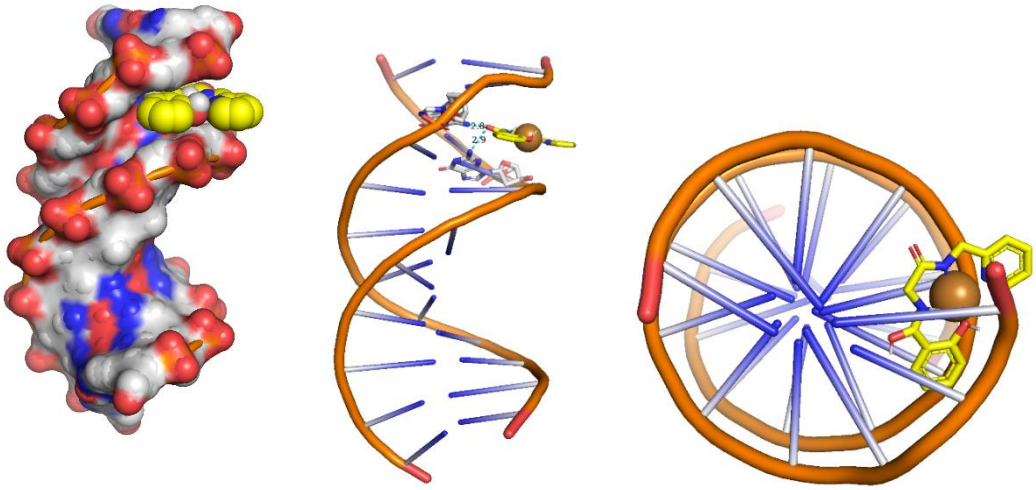

(b)

Figure S22. Docking images of complex **4a** in different viewing modes.

Softare: AutoDock Vina

Binding affinity:-8.1 kcal/mol

Two Hydrogen bonds: $^{\text{Salicylamide}}$C=O-----H-N$^{(\text{Guanine})}$, 2.9Å and 2.8Å

If you used AutoDock Vina in your work, please cite: O. Trott, A. J. Olson, AutoDock Vina: improving the speed and accuracy of docking with a new scoring function, efficient optimization and multithreading, Journal of Computational Chemistry 31 (2010) 455-461 (DOI 10.1002/jcc.21334) Please see http://vina.scripps.edu for more information.

WARNING: The search space volume > 27000 Angstrom^3 (See FAQ)
Detected 8 CPUs
Reading input ... done.
Setting up the scoring function ... done.
Analyzing the binding site ... done.

Using random seed: 2054660232
Performing search ... done.
Refining results ... done.

Table S10. Output data of Autodock analyses **4a**..

mode	affinity (kcal/mol)	dist from best mode rmsd l.b.	rmsd u.b.
1	**-8.1**	**0.000**	**0.000**
2	-8.0	22.221	24.298
3	-7.9	20.223	22.411
4	-7.8	2.069	5.375
5	-7.7	1.970	2.399
6	-7.7	1.905	5.256
7	-7.5	2.490	6.729
8	-7.4	21.857	23.737
9	-7.4	4.005	7.713

Writing output ... done.

(c) Docking of Complex **4c** (SAP3c-Cu**) with** DNA duplex structure (PDB ID 1BNA)

Softare: AutoDock Vina

Binding affinity:-7.9 kcal/mol

Two Hydrogen bonds: $^{\text{Salicylamide}}$C=O-----H-N$^{(\text{Guanine})}$ 2.9Å

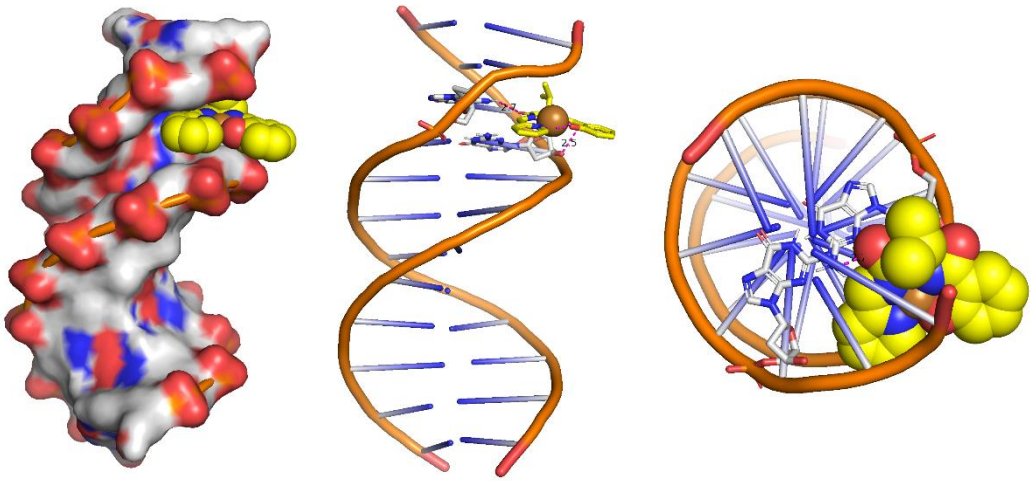

Figure S23. Docking images of complex **4c** in different viewing modes.

Hydrogen bond C=O-----H-N(Guanine), 2.5Å and backbone 2'-Oxygen deoxyribose with salicylic enolic OH (2.8Å)

WARNING: The search space volume > 27000 Angstrom^3 (See FAQ)
Detected 8 CPUs
Reading input ... done.
Setting up the scoring function ... done.
Analyzing the binding site ... done.
Using random seed: 623172056
Performing search ... done.
Refining results ... done.

Table S11. Output data of Autodock analyses **4c**.

mode	affinity (kcal/mol)	dist from best mode rmsd l.b.	rmsd u.b.
1	-7.9	0.000	0.000
2	-7.7	23.770	25.545
3	-7.7	2.379	5.255
4	-7.3	1.395	4.838
5	-7.2	3.057	6.154
6	-7.2	1.911	6.643
7	-7.0	24.506	26.395
8	-7.0	25.962	27.049
9	-6.7	27.114	28.560

Writing output ... done.

Reference

1. O. Trott, A. J. Olson, AutoDock Vina: improving the speed and accuracy of docking with a new scoring function, efficient optimization and multithreading, Journal of Computational Chemistry 31 (2010) 455-461 (DOI 10.1002/jcc.21334)